Breaking boundaries in Electrochemistry: Unveiling a new dimensionless number to tackle convective transfer effect on the voltamperometric answer

Guillaume Hopsort, Cheikhou Kane, Fabien Chauvet, Laure Latapie, Theodore Tzedakis

Electrochemistry Communications 163 (2024) 107706

Contents lists available at ScienceDirect

Electrochemistry Communications

journal homepage: www.elsevier.com/locate/elecom

Breaking boundaries in Electrochemistry: Unveiling a new dimensionless number to tackle convective transfer effect on the voltamperometric answer

Guillaume Hopsort [a], Cheikhou Kane [b], Fabien Chauvet [a], Laure Latapie [a], Theodore Tzedakis [a,*]

[a] Laboratoire de Génie Chimique, Université de Toulouse, CNRS, INPT, UPS, Toulouse, France
[b] Water, Energy, Environment and Industrial Processes Laboratory, École Superieure Polytechnique (ESP), Dakar, Senegal

ARTICLE INFO

Keywords:
Dimensionless number
Electrochemical Engineering
Microfluidics
Steady-transient current transition
Voltammetry response continuity

ABSTRACT

This study introduces the Theokane number (T_k) as a groundbreaking dimensionless number in Electrochemistry. T_k enables the determination of the operating state of an electrochemical (EC) system—indicating whether it is in a transient state (characteristic of cyclic voltammetry) or a steady state (typical of linear sweep voltammetry)—based on a given combination of potential scan rate and residence time. It aims to bridge the gap between various voltamperometric methods. T_k uniquely compares the duration of the potential scan applied to an EC system to the residence time of the reaction mixture at the electrode. This comparison is pertinent in environments ranging from microfluidic setups to macroscale reactors, including stirred vessels.

T_k is particularly crucial for understanding the 'continuous answer' of an EC system subjected to voltamperometric polarization across a spectrum of potential scan and stirring rates. Voltammograms recorded in a micro-reactor under varying conditions highlight the influence of operating parameters on EC responses. The approach introduced in this study accomplish three key objectives: *i)* it validates the T_k number through the comparison of experimental and simulation data, *ii)* it proposes a range for its applicability; and *iii)* it opens a new mode for analyzing EC responses. It is important to note that T_k is applicable to both quasi-reversible and irreversible systems.

1. Introduction

The treatment of the equations describing the physical phenomena is generally derived based on various assumptions. In the realm of electrochemical (EC) methods, this results in a narrow range of validity. Voltammetry constitutes a perfect example: transient state voltammetry, also commonly named Cyclic Voltammetry (CV) at the transient state, requires no fluid motion (or convection) and high potential scan rates ($> \sim 10\ \mathrm{mV.s^{-1}}$). Meanwhile, steady state voltammetry, also commonly known as Linear Sweep Voltammetry (LSV), is performed with solution stirring and low scan rates ($< \sim 5\ \mathrm{mV.s^{-1}}$), often used with Rotating Disk Electrode (RDE) or even Rotating Ring-Disk Electrode (RRDE) [1]. Each method yields specific results and equations, valid only within a restricted range of operating conditions [2]. An analytical approach to studying the transient and steady-state voltammetry of non-reversible electrode processes was conducted by Gonzales et al., specifically focusing on the transition from macroelectrodes to microelectrodes [3].

Electrochemistry lacks generalized parameters that allow for comparing the effects of phenomena across a wide range of operating conditions. Indeed, until now, there is only one dimensionless number specific to EC systems, the Wagner number [4,5], W_a, which compares the effects of the electron transfer resistance to ionic (ohmic) resistance in the solution, on the current distribution into an EC system, as presented by **Eq. (1)**.

$$W_a = \frac{\mathrm{d}\eta}{\mathrm{d}j} \times \frac{\kappa}{\ell} \tag{1}$$

where $\frac{\mathrm{d}\eta}{\mathrm{d}j}$ is the slope of the overpotential-current density curve ($\mathrm{S^{-1}.m^2}$), κ the ionic conductivity of the solution ($\mathrm{S.m^{-1}}$) and ℓ a characteristic length (m).

In voltammetry measurements, the transition between transient and steady states is critical, especially when studying EC reactions coupled to chemical reactions under both regimes. Molina et al. [6] introduced an important parameter the ratio of the transient state peak current I_{ts} to the steady state limiting current I_{ss}, TtSC, defined as $\mathrm{TtSC} = \frac{I_{ts}}{I_{ss}}$.

In this work, we expand the application of this parameter by introducing a new dimensionless number, the Theokane T_k number. The T_k number is designed to describe the continuous behavior of the system in

* Corresponding author.
E-mail addresses: theodore.tzedakis@univ-tlse3.fr, theotzedakis@gmail.com (T. Tzedakis).

https://doi.org/10.1016/j.elecom.2024.107706
Received 6 January 2024; Received in revised form 6 March 2024; Accepted 18 March 2024

Nomenclature

c	Concentration (mol.m^{-3})
D	Diffusion constant (m^2.s^{-1})
E and $E_{I=0}$	Potential and Equilibrium potential (V)
$\mathscr{F}$	Faraday constant
I	Current magnitude (A)
I° and i°	Exchange current and current density (A and A.cm^{-2})
I_a, I_c	Anodic and Cathodic currents (A)
I_{lim}	Current magnitude of the plateau (A)
I_{peak}	Current magnitude of the peak (A)
ℓ	Characteristic length (m)
n	Number of exchanged electron (dimensionless)
N	Mass transfer flux (mol.s^{-1})
p	Pressure (Pa)
q	Volumetric flow rate (m^3.s^{-1})
r	Potential scan rate (V.s^{-1})
Re	Reynolds number (dimensionless)
S_{WE}	Working Electrode Surface area (m^2)
t	Time (s)
T_k	Theokane number (dimensionless)
v	Flow velocity (m.s^{-1})
W_a	Wagner number (dimensionless)

Greek letters

α and β	Anodic and Cathodic exchange coefficients (dimensionless)
$\frac{\Delta I_{ts}-\Delta I_{ss}}{I_{ss}}$	Ratio of the difference between transient and steady state currents to the current at steady state
η	Overpotential (V)
κ	Ionic conductivity (S.m^{-1})
ρ	Density (g.m^{-3})
τ_{res}	Residence time (s)
$\frac{d\eta_c}{dj}$	Slope of the overpotential-current density characteristic (S^{-1}.m^2)

Abbreviations

CE	Counter Electrode
CV	Cyclic Voltammetry
EC	Electrochemical
ECμR	Electrochemical micro-reactor
LSV	Linear Sweep Voltammetry
RDE	Rotating Disk Electrode
RRDE	Rotating Ring-Disk Electrode
TtSC	Transient to Steady Current magnitude ratio
WE	Working Electrode

terms of scan and stirring rates, and even in terms of the flux of electroactive compounds transformed at the interface in the two different operating modes.

The developed theoretical approach is applied to an electrochemical microreactor (ECμR) which allows precise control of flow near electrode surfaces and the recording of voltammograms under a variety of electrode potential scan and flow conditions.

This configuration offers comprehensive insights into system response variations under different scenarios, including transport phenomena and EC reaction limitations.

We also simulate flow, mass transport and EC reactions occurring in the ECμR, comparing these simulations to experimental data. This simulation validates our approach, confirming its reliability and accuracy in predicting the system's behavior.

Finally, this study aims to establish a range of validity for the T_k number. This endeavor is intended to enhance our predictive capabilities regarding the system's response, thereby facilitating more efficient system management and potentially advancing the field of CV.

2. Material and methods

2.1. Material

All the chemicals used in this work were provided by Sigma-Aldrich (USA). Ultra-pure water (18 MΩ.cm) was used to prepare the solutions.

2.2. EC set-up

The EC cell used in this study is a one channel-two streams μ-reactor, double Y-shaped as illustrated in Fig. 1 (~100 μm × 250 μm × 3 cm). The solution used to continuously supply the working electrode (WE) compartment is the ferricyanide $\left[Fe(CN)_6\right]^{3-}$ 5×10^{-3} mol.L^{-1}, in an aqueous solution of KCl 1 mol.L^{-1} (supporting electrolyte avoiding the migration of ferrocyanide). The WE in Pt presents an useful surface of 7.5×10^{-6} m^2. Note that a Pt wire introduced in a dedicated hole near the inlet acts as 'pseudo' reference electrode. A dual-syringe pump was used to feed the reactor.

Depending on the specific case studied, an aqueous solution of KCl 1 mol.L^{-1}, or an aqueous solution of $\left[Fe(CN)_6\right]^{3-}$ 5.10^{-3} mol.L^{-1} + KCl 1 mol.L^{-1} is used to continuously supply the counter electrode (CE, Pt made) compartment of the ECμR.

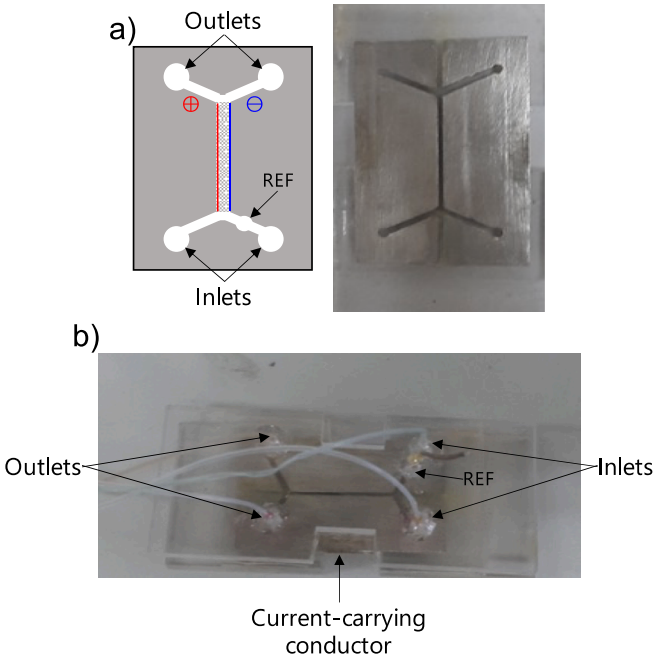

Fig. 1. EC set-up illustrations. a) Schematic view (left) and picture (right) of the working and the counter electrodes, platinum made. b) view of the assembled microreactor.

All solutions supplying the ECμR were deaerated in their storage tank and the same volumetric flow is used for both streams, thanks to a syringe pump. The reaction (2) is involved at the WE surface during the forward scan and the opposite during the backward scan. The solvent reacts on the CE as function of the scan direction.

$$\left[Fe(CN)_6\right]^{3-} + e^- \underset{r_{-1}}{\overset{r_1}{\rightleftharpoons}} \left[Fe(CN)_6\right]^{4-} \quad (2)$$

2.3. Numerical simulation

2.3.1. Geometrical and EC data

The simulations were carried out on COMSOL Multiphysics® software. The exploitation of the simulation results enabled a comparison of the experimental and simulation outcomes. This allowed for the drawing of different curves to characterize hydrodynamics, as well as the verification of certain classic laws in Electrochemistry.

Furthermore, the plotting of $\frac{I_{peak}-I_{lim}}{I_{lim}}$ as a function of the T_k number was carried out for different flow rates for both experimental and numerical determinations.

The geometrical and EC data used in the simulation are presented in Table 1.

2.3.2. Boundary conditions

The flow is modeled by Navier-Stokes equations as presented in **Eqs. (3)–(4)**.

$$\rho \frac{\partial \vec{v}}{\partial t} = -\nabla p + \nabla \bullet \tau \quad (3)$$

$$\nabla . \vec{v} = 0 \quad (4)$$

where ρ is the (mass) density (g.m^{-3}), $\vec{v}$ is the flow velocity (m.s^{-1}), t is time (s), p is the pressure (Pa), τ is the stress tensor.

At the inlet of the system, the average velocity is deduced from the flow rate. Along the system's walls, the no-slip condition is applied. At the outlet, the relative pressure is assumed to be zero.

In the study of convection–diffusion under transient conditions, the governing equation is represented by **Eq. (5)**.

$$\frac{\partial c}{\partial t} = \nabla \bullet (D \nabla c) - \vec{v} \nabla c \quad (5)$$

here, c represents the concentration (mol.m^{-3}).

At the microchannel's entrance, the concentration of the ferricyanide is 5 mmol.L^{-1}. On all walls, except on the electrode, an insulation boundary condition is applied, signifying no mass transfer through these walls.

On the electrode, the mass transfer flux (N, mol.s^{-1}) is defined by **Eq. (6)**.

$$N = \frac{I}{n\mathscr{F}} \quad (6)$$

where $\mathscr{F}$ denotes the Faraday constant (96,500 C.mol^{-1}), n is the number of exchanged electrons (dimensionless, equal to 1 in the case of reaction (2)). I represents the net current, which is the difference between the anodic partial current (I_a) and the partial cathodic current (I_c). The current magnitude follows the Butler-Volmer law and can be expressed in terms of the overpotential ($\eta = E - E_{I=0}$) as shown in **Eqs. (7)–(8)**.

Table 1
Geometrical and EC data used for numerical determination.

Microchannel dimensions (μm)	~ 100 μm × 250 μm × 3 cm
Diffusion constant D (m^2.s^{-1}) [7]	7.6×10^{-10}
Exchange current density i° (A.cm^{-2}) [8]	9
Initial ferricyanide concentration (mmol.L^{-1})	5
Hydraulic diameter (μm)	143
Kinematic viscosity[9] (cm^2.s^{-1})	9
Anodic exchange coefficient [8]α	0.4
Cathodic exchange coefficient [8]β	0.6

$$I = I^\circ \times \left\{ \frac{c_{red,elec}}{c_{red,bulk}} \times \exp\left[\frac{\alpha n \mathscr{F} \eta}{RT}\right] - \frac{c_{o,elec}}{c_{o,bulk}} \times \exp\left[\frac{-\beta n \mathscr{F} \eta}{RT}\right] \right\} \quad (7)$$

$$I = I^\circ \times \left\{ \left|\frac{I_{lim}^{an} - I^{an}}{I_{lim}^{an}}\right| \times \exp\left[\frac{\alpha n \mathscr{F} \eta}{RT}\right] - \left|\frac{I_{lim}^{cath} - I^{cath}}{I_{lim}^{cath}}\right| \times \exp\left[\frac{-\beta n \mathscr{F} \eta}{RT}\right] \right\} \quad (8)$$

where $E_{I=0}$ refers to the equilibrium potential (V), T is the temperature (K), R is universal gas constant (8.31 J.K^{-1}.mol^{-1}), $c_{o,bulk}$ and $c_{red,bulk}$ are the concentration of the species to be oxidized and to be reduced, respectively (mol.m^{-3}) and $c_{o,elec}$ and $c_{red,elec}$ are the concentration at the surface of the electrode of oxidant and reductant, respectively (mol.m^{-3}).

The potential E varies according to **Eq. (9)** depending on the oxidation or reduction reactions.

$$E = E_{I=0} \pm r \times t \quad (9)$$

At the system's outlet, the flux is convective (normal diffusion flux = 0), indicating that the transport of species is primarily due to the movement of the fluid itself.

3. Results

3.1. The T_k number

The Theokane number T_k compares the characteristic time of an electrode potential variation applied to a system to the residence time of the reaction mixture within that system. T_k is defined in **Eq. (10)** as the ratio of the time required to complete one potential scan to the residence time of the flowing mixture in the reactive area.

$$T_k = \frac{t_{\Delta E}}{\tau_{res}} = \frac{\Delta E}{r} \times \frac{q}{V_{EC}} = \frac{\Delta E \times \vec{v}}{r \times \ell} \quad (10)$$

Here, $t_{\Delta E}$ represents the time needed to complete one potential scan, either forward or backward, from the initial $E_{initial}$ to the final E_{final} potential (where $\Delta E = E_{initial} - E_{final}$). The residence time τ_{res} is the time the electroactive compound(s) spend in the system.

$t_{\Delta E}$ can also be expressed as the ratio of ΔE, the studied potential window (V), to the potential scan rate r (V.s^{-1}).

For the residence time τ_{res}, this parameter is evaluated as the ratio of the volumetric flow rate q (m^3.s^{-1}) to the volume of the involved EC system V_{EC} (m^3). Similarly, the volumetric flow rate q is the product of the cross-sectional area of the flow channel and the average flow velocity $\vec{v}$ (m.s^{-1}).

The volume V_{EC} varies depending on the type of EC reactor:

- in an ECμR's electrolyte compartment, V_{EC} is the microchannel volume, corresponding to the channel cross-section x length of the channel ℓ (m);
- in a stirred vessel, V_{EC} is equal to the product of the cross-sectional area of the diffusion layer and its thickness (also noted ℓ).

T_k aims to elucidate the continuity in the voltamperometric response of an EC system transitioning from steady state to transient state, thereby bridging the gap between different voltammetric methods (*e.g.*, CV and LSV).

Strictly speaking, T_k approaches zero for completely immobilized solutions (where $\vec{v}$ approaches zero), which, at first glance, might be attributed to a perfect example of transient state voltammetry. This scenario arises solely when the EC reaction involves a 'simple exchange of one electron without any change in the physical state of the reagent'. More commonly, the EC reaction itself induces convective motion near the interface due to changes in the solution's density. Conversely, when potential scan rates are slow (r approaches zero), T_k tends towards infinity, a condition that could be associated with steady state

voltammetry. Both of these situations represent extreme cases in which T_k cannot be explicitly utilized.

Currently, various works focused on quasi-reversible systems (fast electron transfer) [10,11], but T_k is also applicable to irreversible systems. Voltametric measurements were conducted using microfluidic device (an undivided ECμR) under variable conditions, highlighting the effects of flow and potential scan rate on the current–potential $I = f(E)$ curves.

However, the approach is applicable to any EC system, including for example stationary and rotating electrodes in batch systems.

3.2. Effect of the potential scan rate

Fig. 2 displays the voltammograms obtained from a double Y-shaped ECμR (refer to the method section for details), operated under a constant flow rate of 750 μL.min^{-1} (30 m.min^{-1}) using an aqueous ferricyanide solution. The experiments were conducted at different potential scan rates. In these voltammograms, the cathodic section, which represents the reduction of $Fe^{(III)}$, is of particular interest. For high potential scan rates r (greater than 50 mV.s^{-1}), the curves are peak shaped, indicating the transient nature of the current. However, as r decreases, the peak current magnitude also decreases, and the curve evolves into a monotonic shape with a plateau. This plateau corresponds to the limiting current (I_{lim}). It should be noted that the observed increase in current at −0.2 V corresponds to the reduction of residual dissolved oxygen.

3.3. Effect of the volumetric flow

Fig. 3 illustrates the impact of flow rate on the $I = f(E)$ curves, obtained using the same double Y-shaped ECμR, as in Fig. 1, but at a fixed potential scan rate of 5 mV.s^{-1}. At higher flow rates, the curve exhibits a diffusion plateau, indicating a steady state of mass transport phenomena at the interface, where convection sufficiently renews the composition at the electrode surface. As the flow rate decreases, the electroactive compound is fully consumed at electrode surface (concentration ~0) causing the current to fall and resulting in a peak-shaped curve. It is notable that higher flow rates correlate with higher limiting current value. The peak current reflects the dynamic (transient) nature of the diffusional layer near the electrode surface.

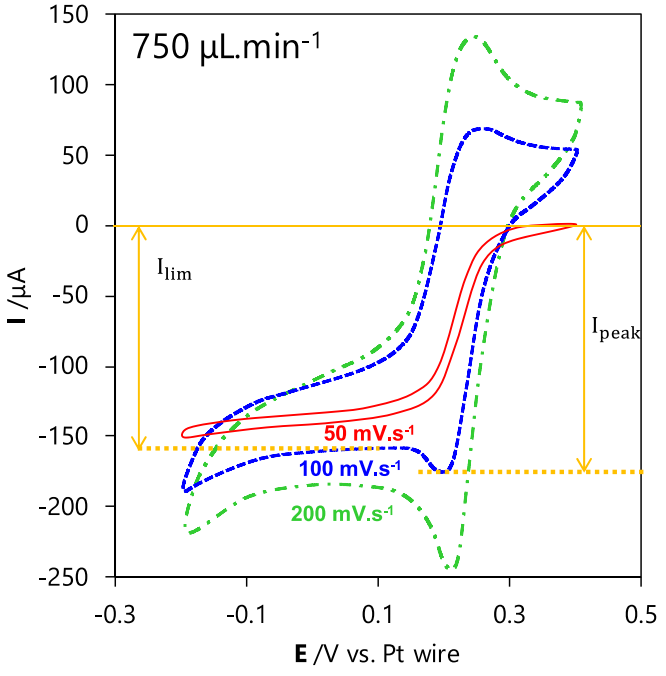

Fig. 2. Voltammograms obtained in a double Y-shaped ECμR, using a 5×10^{-3} mol.L^{-1} ferricyanide $[Fe(CN)_6]^{3-}$ solution in 0.1 mol.L^{-1} KCl electrolyte, flowing at 750 μL.min^{-1}. Microchannel dimensions: 100 μm × 250 μm × 3 cm. Surface area of the working electrode: 7.5×10^{-6} m^2. The working electrode was initially submitted to a cathodic polarization. Curves were plotted for different potential scan rates: 50 (red, solid line), 100 (blue, dashed line) and 200 mV.s^{-1} (green, dotted line).

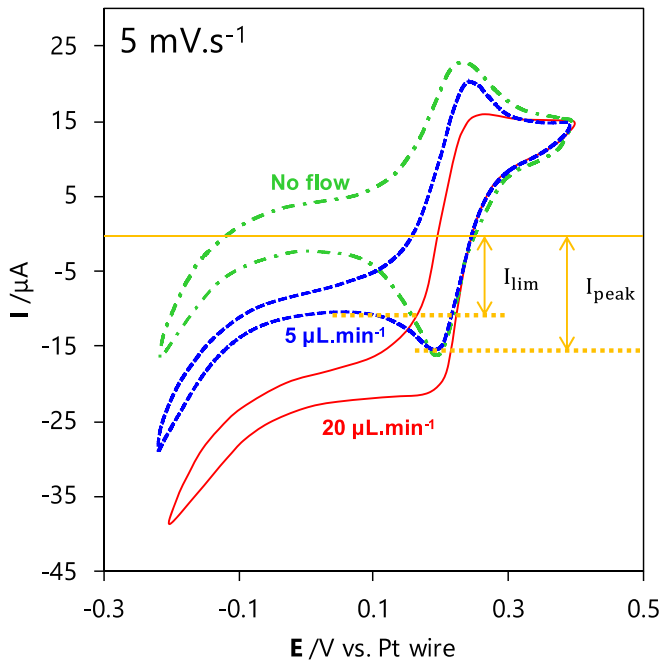

Fig. 3. Voltammograms obtained in a double Y-shaped ECμR, using a 5×10^{-3} mol.L^{-1} ferricyanide $[Fe(CN)_6]^{3-}$ solution in 0.1 mol.L^{-1} of KCl electrolyte. Microchannel dimensions: 100 μm × 250 μm × 3 cm. Surface area of the working electrode: 7.5×10^{-6} m^2. The working electrode was initially submitted to a cathodic polarization at 5 mV.s^{-1}. Curves were plotted for potential flow rates at 0, 5 and 20 μL.min^{-1} (0.02 to 0.83 m.min^{-1}).

3.4. Transition between steady and transient state currents: T_k evolution

The T_k dimensionless number enables determining the operating state of an EC system – whether it is in a transient state (characteristic of CV) or a steady state (typical of LSV) –for a given combination of potential scan rate and residence time. A decrease in T_k indicates an increase in residence time relative to the potential scan time, leading the system to exhibit CV curves characteristic of the transient state. Conversely, as T_k increases, the system tends to produce LSV curves with a diffusion plateau and limiting current I_{lim}, indicative of stationary voltammetry without transient effects.

Fig. 4-**a** illustrates the $\frac{(I_{peak}-I_{lim})}{I_{lim}} = (TtSC-1) = f(T_k)$ curves for various volumetric flow rates and potential scan rates.

At the same potential scan rate, the transient state occurs at low flow rates, marked by a significant difference between I_{peak} and I_{lim}. When $\frac{(I_{peak}-I_{lim})}{I_{lim}}$ is plotted as a function of T_k, all curves align on the same trajectory, as shown in Fig. 4-**b**. The inset of Fig. 4-**a** suggests that diffusive fluxes predominate when $T_k < 1$, while convective fluxes prevail when $T_k > 10$.

The measured current can be expressed as the sum of two terms: I_{peak} and I_{lim}. The first term represents the molar flux of the oxidizer electroreduced near the interface before the diffusion layer is established, while the second term corresponds to the limiting current due to mass transport limitation across the fully developed diffusion layer.

Traditionally in Electrochemistry, I_{peak} is assumed [12,13] to be a power law function of the potential scan rate r as in **Eq. (11)**.

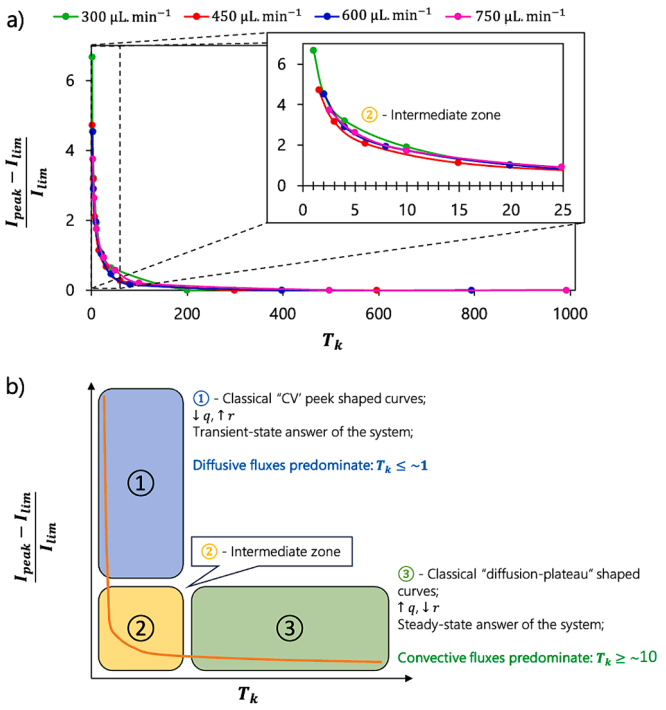

Fig. 4. Comprehensive voltammetric response of an EC system, analyzed through the T_k number. a) Curves $\frac{(I_{peak}-I_{lim})}{I_{lim}} = f(T_k)$ for different flow rates ranging from 300 to 750 µL.min^{-1} (12 to 30 m.min^{-1}) and potential scan rates from 5 to 200 mV.s^{-1}, b) a schematic depiction of the system's behavior as a function of the T_k number.

$$I_{peak} = k_1 \times r^{0.5} = k_1 \times \left(\frac{\Delta E}{t_{\Delta E}}\right)^{0.5} \tag{11}$$

where k_1 is a constant.

Similarly, the classical Lévêque [14] or Lee et al. [15,16] correlations allow the limiting current to be expressed as a power law of the flow rate q and, consequently, of the velocity ν of the electrolyte within the electrode-delimiting channel as in **Eq. (12)**.

$$I_{lim} = k_2 \times \nu^{\alpha} \tag{12}$$

with k_2 a constant and α an exponent influenced by the reactor's geometry.

The transient to steady current magnitudes ratio can be expressed based on the above equations as in **Eq. (13)**.

$$\frac{I_{peak}-I_{lim}}{I_{lim}} = \frac{k_1 \times r^{0.5}}{k_2 \times \nu^{\alpha}} - 1 \tag{13}$$

After rearranging, it becomes **Eq. (14)**.

$$\frac{I_{peak}-I_{lim}}{I_{lim}} + 1 = \frac{k_1}{k_2} \times r^{0.5-\alpha} \times \left(\frac{r}{\nu}\right)^{\alpha} = \frac{k_1}{k_2} \times r^{0.5-\alpha} \times \left(\frac{\Delta E}{\ell}\right)^{\alpha} \times T_k^{-\alpha} \tag{14}$$

where ℓ is a characteristic length of the reactor (m).

Plotting, $ln\left(\frac{I_{peak}-I_{lim}}{I_{lim}}+1\right)$ as function of ln (T_k) at a constant potential scan rate r results in a straight master line, as depicted in Fig. 5 for all examined potential scan rates.

This linearity demonstrates the continuity of the response of the EC system, obeying to **Eq. (15)**.

$$\ln\left(\frac{I_{peak}-I_{lim}}{I_{lim}}+1\right) = \ln\left(\frac{k_1}{k_2} \times r^{0.5-\alpha} \times \left(\frac{\Delta E}{\ell}\right)^{\alpha}\right) - \alpha \times \ln(T_k) \tag{15}$$

As depicted in Fig. 5, the 'common' slope of this function leads to the

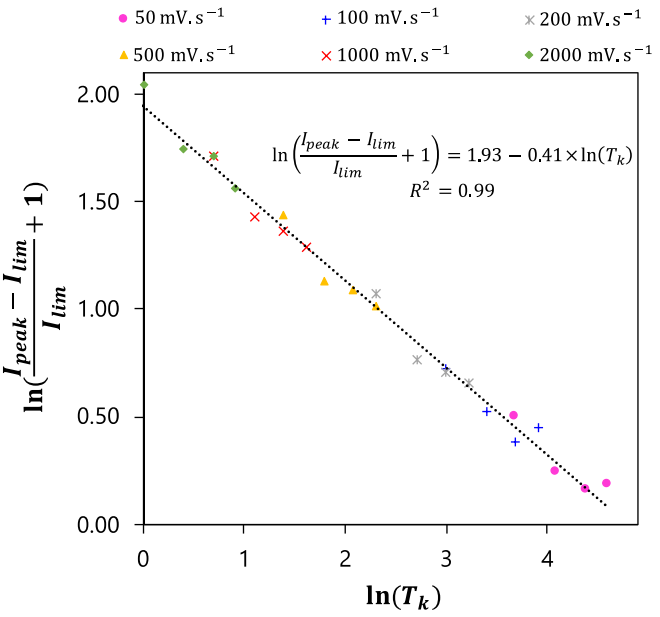

Fig. 5. Comparative analysis of voltammetric responses according to $\ln\left(\frac{I_{peak}-I_{lim}}{I_{lim}}+1\right) = f(\ln(T_k))$ at various potential scan rates ranging from 50 to 2000 mV.s^{-1} and flow rates from 300 to 750 µL.min^{-1}. The observed linear trends underscore the system's consistency and predictability under varying EC conditions.

coefficient $\alpha = 0.4$, a value consistent with standards found in the Chemical Engineering correlations [17–19].

3.5. Modelling and simulation of convection–diffusion phenomena

As presented in the Methods section, the EC process within the ECµR was simulated by numerically solving equations for flow, mass transport, and EC reactions.

An example of numerically obtained voltammograms at high flow (1500 µL.min^{-1}) and various potential scan rates is shown in Fig. 6-a. These curves exhibit the main characteristics of the experimental curves presented in Fig. 2.

Fig. 6-b illustrates the experimental (solid blue curve) and numerical (green dashed curve) evolutions of the ratio $\frac{(I_{peak}-I_{lim})}{I_{lim}}$ as a function of T_k.

As previously indicated, the simulation confirms a rapid decrease in the transient to steady current magnitude ratio (TtSC-1) for $T_k \leq 1$ (where diffusion limitation predominates), and a lower dependence on the current's ratio for $T_k \geq 10$ (where convection limitation predominates). A maximum deviation of 1 % is found between the resolution and the experimental value, validating the numerical model.

Fig. 6-c and d illustrate the evolution of ferricyanide concentration during the reduction and oxidation cycles of ferricyanide, occurring within the 'working electrode channel', over the period between the inlet and outlet times (equivalent to one residence time). More specifically, Fig. 6-c reveals that, during one residence time, five cycles take place: the concentration of ferricyanide decreases due to consumption *via* reduction, and subsequently increases as a result of regeneration *via* oxidation. An important observation pertains to the trend in the concentration of the regenerated ferricyanide: it shows a continuous decrease from 5 to 3.5 mmol.L^{-1}. This diminution is attributed to the low flow rate and the ensuing diffusion towards the counter electrode compartment, which contains only KCl.

Conversely, for higher Theokane number values ($T_k = 10$, Fig. 6-d), no changes in concentration were observed during the scans. This is attributed to the low residence time, which consequently minimizes the

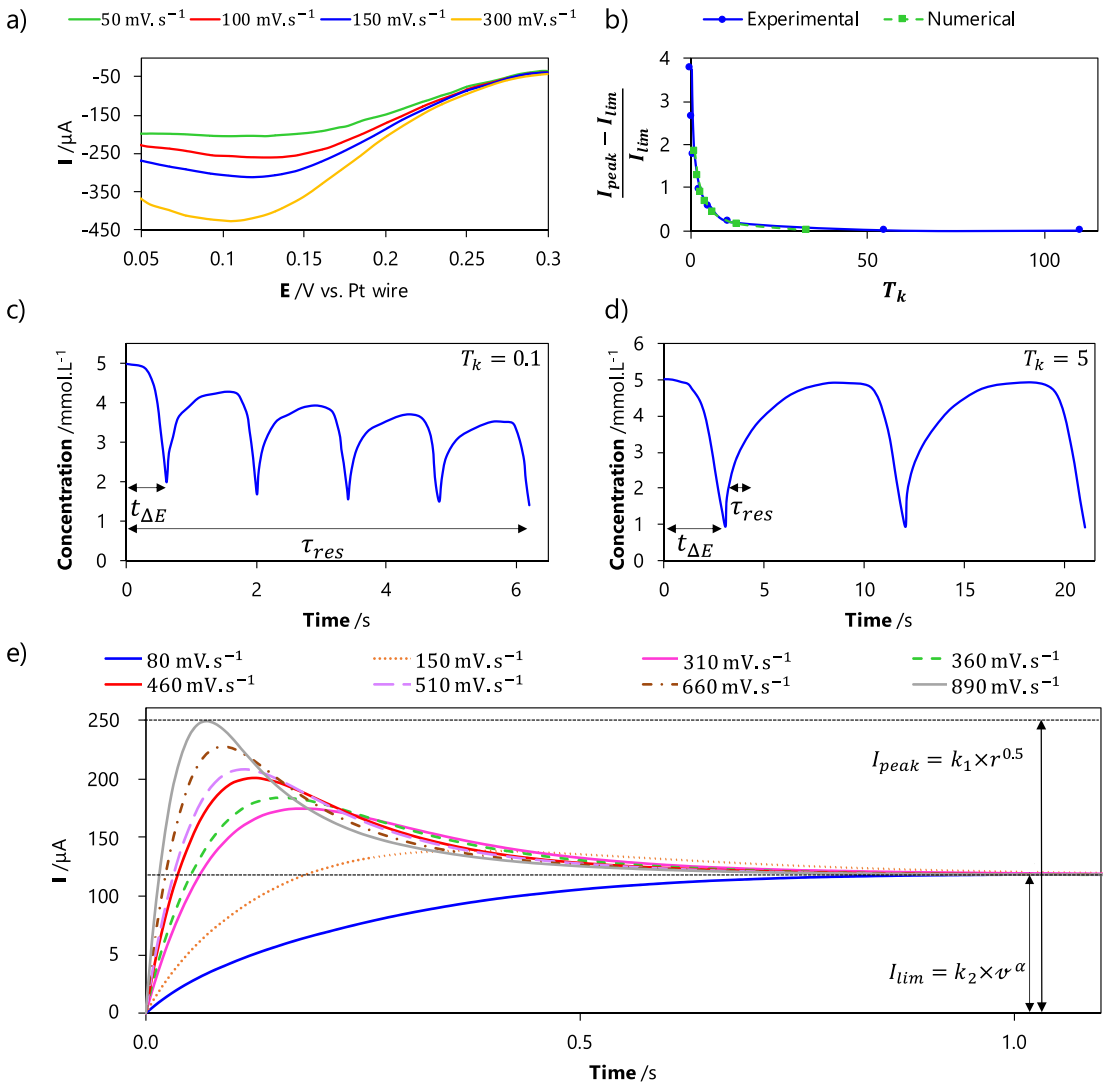

Fig. 6. Numerical results obtained for ferricyanide system modeling to validate the T_k dimensionless number (assuming ferricyanide as a perfectly reversible redox system). a) Numerically obtained voltammograms in a double Y-shaped (two streams, one channel ~ 100 µm × 250 µm × 3 cm, $S_{WE} = 7.5 \times 10^{-6}$ m^2) ECµR using a 5×10^{-3} mol.L^{-1} ferricyanide $[Fe(CN)_6]^{3-}$ solution in 0.1 mol.L^{-1} of KCl electrolyte at 1500 µL.min^{-1}, for various potential scan rates from 50 to 300 mV.s^{-1}. b) Comparison of $\frac{(I_{peak}-I_{lim})}{I_{lim}} = f(T_k)$ curves between numerical and experimental data at a flow rate of 1500 µL.min^{-1}. c) Electrode concentration variation at one residence time, $T_k = 0.1$, $r = 500$ mV.s^{-1} and $q = 113.4$ µL.min^{-1}, Re = 2.42. d) Electrode concentration variation, $T_k = 5$, $r = 100$ mV.s^{-1} and $q = 1134$ µL.min^{-1}, Re = 24.2. e) Simulated temporal current evolution in the ECµR at various potential scan rates from 80 to 890 mV.s^{-1}, and at an average flow velocity v = 3 cm.s^{-1}.

interdiffusion flux between both streams.

Fig. 6-e presents the theoretical voltamperometric response of the system (assuming ferricyanide as a perfectly reversible redox system) as a function of time for large-scale values of potential scan rates. It suggests that the current reaches a steady state constant value, i.e. 'the limiting current' (mass transfer limitation across the fully developed diffusion layer).

The first peak area (t< ~ 0.3 s) represents the molar flux of the oxidizer electro-reduced near the interface before the diffusion layer's establishment.

4. Conclusion

In conclusion, this research introduces the Theokane number (T_k), an innovator dimensionless number in Electrochemistry, which enables bridging the conceptual and operational divide between different voltammetry techniques. The T_k number, by comparing the action time to the residence time in an EC system, allows easy characterization of the system's behavior under a range of potential scan and stirring rates. The innovative approach allows to analyze the EC processes, overcoming the limitations of traditional methods that often overlook the complexities of mass and electron transfer.

The practical applications of the T_k number were rigorously tested through a series of experiments using a ECµR, where voltammograms were recorded under diverse conditions of flow rate and potential scan rate. Results from these experiments, coupled with our modeling and simulation efforts, not only validated the T_k number but also helped in establishing a scale for its effective utilization:

$$1\ (\textit{for diffusive fluxes predominance, transient state EC methods}) \geq T_k \geq 10\ (\textit{for convective fluxes predominance, steady state EC methods})$$

This study's significance lies in its potential to enhance the predictive response of EC system, thereby facilitating better system management and potentially driving innovation in voltammetry. The T_k number's applicability to both quasi-reversible and non-reversible systems further underscores its versatility and utility in advancing the field of Electrochemistry. Our research paves the way for future studies to explore and expand upon the fundamental concepts introduced here, promising a more comprehensive and integrated approach to EC analysis.

CRediT authorship contribution statement

Guillaume Hopsort: Writing – review & editing, Writing – original draft, Visualization, Formal analysis, Data curation. **Cheikhou Kane:** Validation, Investigation, Formal analysis, Data curation. **Fabien Chauvet:** Validation, Methodology, Investigation, Data curation. **Laure Latapie:** Data curation. **Theodore Tzedakis:** Writing – review & editing, Writing – original draft, Visualization, Formal analysis, Methodology, Investigation, Validation.

Declaration of competing interest

The authors declare that they have no known competing financial interests or personal relationships that could have appeared to influence the work reported in this paper.

Data availability

Data will be made available on request.

Acknowledgements

This study is supported by recurrent founds from Université Toulouse III – Paul Sabatier.

References

[1] R.G. Compton, S.V. Sokolov, Electrochemistry needs electrochemists: "goodbye to rotating discs", J. Solid State Electrochem. (2023) https://doi.org/10.1007/s10008-023-05443-8.
[2] G. Bontempelli, R. Toniolo, MEASUREMENT METHODS | Electrochemical: Linear Sweep and Cyclic Voltammetry, in: Encycl. Electrochem. Power Sources, Elsevier, 2009: pp. 643–654. https://doi.org/10.1016/B978-044452745-5.00069-1.
[3] J. Gonzalez, A. Molina, F. Martinez-Ortiz, M. Lopez-Tenes, R.G. Compton, Analytical approach to the transient and steady-state Cyclic Voltammetry of non-reversible electrode processes Defining the transition from macro to microelectrodes, Electrochimica Acta 213 (2016) 911–926, https://doi.org/10.1016/j.electacta.2016.07.145.
[4] S. Li, Chapter 13 - Introduction to Electrochemical Reaction Engineering, in: React. Eng., Butterworth-Heinemann, Boston, 2017: pp. 599–651. https://doi.org/10.1016/B978-0-12-410416-7.00013-6.
[5] K.R. Kim, S.K. Kim, J.G. Kim, H.O. Nam, CFD approach to wagner number estimation for a current distribution uniformity in a rotating cylinder hull cell, Int. J. Electrochem. Sci. 13 (2018) 8686–8693, https://doi.org/10.20964/2018.09.73.
[6] Á. Molina, J. González, C.M. Soto, M. López-Tenés, Transient and steady state behaviour of electrochemical reactions preceded by a chemical step at spherical electrodes: A chronopotentiometric study, J. Electroanal. Chem. 645 (2010) 74–80, https://doi.org/10.1016/j.jelechem.2010.04.017.
[7] J.E. Baur, R.M. Wightman, Diffusion coefficients determined with microelectrodes, J. Electroanal. Chem. Interfacial Electrochem. 305 (1991) 73–81, https://doi.org/10.1016/0022-0728(91)85203-2.
[8] M. Spiro, Standard exchange current densities of redox systems at platinum electrodes, Electrochimica Acta 9 (1964) 1531–1537, https://doi.org/10.1016/0013-4686(64)85032-5.
[9] N.P.C. Stevens, M.B. Rooney, A.M. Bond, S.W. Feldberg, A comparison of simulated and experimental voltammograms obtained for the [Fe(CN)6]3-/4- couple in the absence of added supporting electrolyte at a rotating disk electrode, J. Phys. Chem. A 105 (2001) 9085–9093, https://doi.org/10.1021/jp0103878.
[10] D.J. Gavaghan, A.M. Bond, A complete numerical simulation of the techniques of alternating current linear sweep and cyclic voltammetry: analysis of a reversible process by conventional and fast Fourier transform methods, J. Electroanal. Chem. 480 (2000) 133–149, https://doi.org/10.1016/S0022-0728(99)00476-3.
[11] P. Zhao, S. Yun, Z. Hu, D. Qi, Quantitative analysis of a mixture with reversible electrode processes by cyclic voltammetry and linear sweep voltammetry, J. Electroanal. Chem. 402 (1996) 11–17, https://doi.org/10.1016/0022-0728(95)04214-8.
[12] N. Elgrishi, K.J. Rountree, B.D. McCarthy, E.S. Rountree, T.T. Eisenhart, J. L. Dempsey, A practical beginner's guide to cyclic voltammetry, J. Chem. Educ. 95 (2018) 197–206, https://doi.org/10.1021/acs.jchemed.7b00361.
[13] A.J. Bard, L.R. Faulkner, Electrochemical methods: fundamentals and applications, 2. edition, Wiley, New York Weinheim, 2001.
[14] J. Newman, N.P. Balsara, Electrochemical systems, Fourth edition, Wiley, Hoboken, NJ, 2021.
[15] H.-J. Lee, F. Sarfert, H. Strathmann, S.-H. Moon, Designing of an electrodialysis desalination plant, Desalination 142 (2002) 267–286, https://doi.org/10.1016/S0011-9164(02)00208-4.
[16] H.-J. Lee, H. Strathmann, S.-H. Moon, Determination of the limiting current density in electrodialysis desalination as an empirical function of linear velocity, Desalination 190 (2006) 43–50, https://doi.org/10.1016/j.desal.2005.08.004.
[17] X. You, Q. Ye, P. Cheng, The dependence of mass transfer coefficient on the electrolyte velocity in carbon felt electrodes: determination and validation, J. Electrochem. Soc. 164 (2017) E3386–E3394, https://doi.org/10.1149/2.0401711jes.
[18] K.J. Min, J.H. Kim, K.Y. Park, Characteristics of heavy metal separation and determination of limiting current density in a pilot-scale electrodialysis process for plating wastewater treatment, Sci. Total Environ. 757 (2021) 143762, https://doi.org/10.1016/j.scitotenv.2020.143762.
[19] J.-Y. Chen, C.-L. Hsieh, N.-Y. Hsu, Y.-S. Chou, Y.-S. Chen, Determining the limiting current density of vanadium redox flow batteries, Energies 7 (2014) 5863–5873, https://doi.org/10.3390/en7095863.